

# MODEL OF THE CANTILEVER USED AS A WEAK FORCE SENSOR IN ATOMIC FORCE MICROSCOPY

Michal Hrouzek <sup>\*,1</sup> Alina Voda <sup>\*</sup> Martin Stark <sup>\*\*</sup>  
Joël Chevrier <sup>\*\*\*</sup>

<sup>\*</sup> *Le Laboratoire d'Automatique de Grenoble – INPG,  
BP. 46, 38402 Saint Martin d'Hères, France*

<sup>\*\*</sup> *Laboratoire de Spectrométrie Physique – UJF, BP. 87,  
38402 Saint Martin d'Hères, France*

<sup>\*\*\*</sup> *LEPES – C.N.R.S., 25 Avenue des Martyrs, BP. 166,  
38000 Grenoble Cedex, France*

Abstract: New types of weak forces measurements with Atomic Force Microscope (AFM) are very challenging for experimental physics and call for new studies on control strategies operating the AFM. It is thus necessary to first develop a precise model of the cantilever with its sharp tip, in interaction with the scanned sample. This paper presents a model of the cantilever, that is based on beam theory and taking into account the influence of the long distance interaction forces. *Copyright ©2005 IFAC*

Keywords: Microscopes, Microsystems, Models

## 1. INTRODUCTION

Atomic Force Microscopy (AFM) is one example of Scanning Probe Microscopy (SPM), which is capable of measuring the interaction force between the sample and a sharp tip mounted on the end of a soft cantilever (usually made of silicon with rectangular or triangular shape). The topography of the surface and many other properties can be determined from the measured forces.

The AFM is a very complex instrument that incorporates broad control systems responsible for excitation of the cantilever with mounted tip and positioning of the measured sample underneath it. New applications of the AFM require improvements in measurement accuracy. As a main limitation of achievable measurement sensitivity is

thermal noise (Butt and Jaschke, 1995)(Giessibl, 1997). Thermally excited cantilever and its random movement around its equilibrium position is contributing in the total displacement of the lever during scanning of the measured surface (M.Ashhab *et al.*, 1999). This is very critical for new experiments in physics, like weak force measurements and nano-manipulation. Therefore, there is a need for new control strategies that can deal with the thermal noise. At the present time the standard control strategies for the cantilever excitation are based on PI, PID controllers, which give limited performance. Even if advanced control of AFM has been already proposed for the excitation, the thermal noise is still limiting the measurement accuracy.

Development of control systems that are responsible for treading the thermal noise excitation are asking for precise model of the cantilever in the interaction with the surface and the influence of

---

<sup>1</sup> Partially supported by University of Technology Brno, Czech republic

the thermal noise in this system. The beam theory is describing the behavior of the cantilever as a clamped beam (Clough and Penzien, 1993) and is capable to determine the contribution of higher harmonics. This paper consider higher complexity modeling of the cantilever, validated by practical experiments.

## 2. CANTILEVER MODEL

Models are usually used for simulation of specific properties of the levers and/or interactions. Often used models are based on simple mechanical principles with a description as a second order differential equation for the position of the free end. Vibrating cantilever is described as a simple oscillator with mass  $m$  attached to a spring with stiffness  $k$  and a dashpot characterized by its damping constant  $\gamma$ . The movement of the lever is affected by external forces: the driving force from the piezo bimorph  $F_{dri}$ , the interaction force  $F_{int}$  and all perturbation forces  $F_{per}$ .

A better description of the free cantilever vibrations comes from the beam theory, which is describing the movement of the lever very precisely (Clough and Penzien, 1993) (Rast *et al.*, 2000). The cantilever is described as a beam clamped at one end, while the other end is freely vibrating. This description includes different modes of vibrations at their specific resonance frequencies. The mathematical description of the movement is based on the one-dimension Euler-Bernoulli equation that fully describes the dynamics of the rectangular cantilever (Clough and Penzien, 1993). The equations describing the system wouldn't be so complex if it is assumed that all the significant physical properties are constant along the span of the beam. This means that the moment of inertia  $I(x)$ , Young's modulus  $E(x)$ , the mass per unit length  $\bar{m}(x)$ , and the cross section need to be constant everywhere on the cantilever.

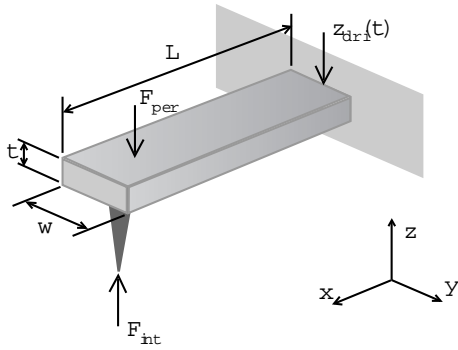


Fig. 1. Schematic of the cantilever mechanical properties.

Most cantilevers used in AFM are rectangular at their cross sections. The mathematical description

of free vibration for this system is described by differential equation of fourth order:

$$EI \frac{\delta^4 v(x,t)}{\delta x^4} + \bar{m} \frac{\delta^2 v(x,t)}{\delta t^2} = 0 \quad (1)$$

where  $v(x,t)$  is the time dependent transverse displacement from the neutral position at position  $x$ . The solution for Eq. 1 can be obtained easily by separation variables, using the substitution  $v(x,t) = \phi(x)Y(t)$ . Expressing transformed function 1 in terms of trigonometric and hyperbolic functions and setting the entire imaginary part to zero leads to the solution

$$\phi(x) = A_1 \cos \alpha x + A_2 \sin \alpha x + A_3 \cosh \alpha x + A_4 \sinh \alpha x \quad (2)$$

where  $A_1$ ,  $A_2$ ,  $A_3$ , and  $A_4$  are real constants and  $\alpha$  is parameter for existing harmonic mode. The parameters can be found with the help of boundary and linking conditions. Freely vibrating beam fixed on one side fulfills four boundary conditions. The first two conditions are a consequence of fixing the cantilever in displacement and inclination to the driver at  $x=0$ . At the fixed end the deflection is zero  $\phi(0) = 0$  and also the slope  $\phi'(0) = 0$ . The third boundary condition claims that at  $x=L$  the torque force vanishes  $EI\phi''(L) = 0$  (zero bending). The fourth condition means that the external force is zero at the end of the cantilever  $EI(L)\phi''' = 0$  (zero shear). Equation 2 have non zero solution that has to fulfill condition  $\cos \alpha_i = -(1/\cosh \alpha_i)$ , numerical solution is  $\alpha_1 = 1.875$ ,  $\alpha_2 = 4.694$ ,  $\alpha_3 = 7.855$ ,  $\alpha_4 = 10.996$ ,  $\alpha_i \doteq (i - 1/2)\pi$  for  $i \geq 5$ . The corresponding circular frequency for a given solution  $i$  can be obtained as shown by

$$\omega_i = \alpha_i^2 \sqrt{\frac{EI}{\bar{m}L^4}} \quad (3)$$

where  $i=1,2,3, \dots$  is the index of the resonant frequency for a particular vibration mode. Now  $A_2$  can be determined from the boundary conditions as a function of  $A_1$  for harmonic solutions with specific harmonic frequencies  $\omega_i$ . The solution of 1 can be expressed as in 4, where each term in the sum represents a vibration mode. It is the product of a time dependent function  $\sin(\omega_i t)$  and a function  $\phi_i(x)$  which only depends on the position  $x$  along the cantilever.  $C_i$  is the amplitude of a certain vibration mode. The phase shifts  $\delta_i$  depend on the initial state (deflection, velocity) of the cantilever only.

$$z = \sum_{i=1}^{\infty} C_i \sin(\omega_i t + \delta_i) \phi_i(x)$$

$$\phi_i(x) = (\sin \alpha_i + \sinh \alpha_i) \left( \cos \frac{\alpha_i}{L} x - \cosh \frac{\alpha_i}{L} x \right)$$

$$- (\cos \alpha_i + \cosh \alpha_i) \left( \sin \frac{\alpha_i}{L} x - \sinh \frac{\alpha_i}{L} x \right) \quad (4)$$

The multi mode cantilever model can be described as a linear time invariant system (Stark *et al.*, 2004) defined by its matrix of dynamics  $\mathbf{A}$ , matrix of inputs  $\mathbf{B}$ , matrix of output  $\mathbf{C}$  and feed through matrix  $\mathbf{D}$ .

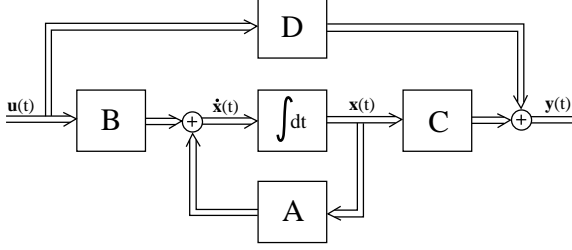


Fig. 2. Linear time time invariant model of the cantilever.

$$\dot{\mathbf{x}}(t) = \mathbf{A}\mathbf{x}(t) + \mathbf{B}\mathbf{u}(t) \quad (5)$$

$$\mathbf{y}(t) = \mathbf{C}\mathbf{x}(t) + \mathbf{D}\mathbf{u}(t) \quad (6)$$

where  $\mathbf{u}(t)$  is an input vector,  $\dot{\mathbf{x}}(t)$  is state derivation vector,  $\mathbf{x}(t)$  is a state vector,  $\mathbf{y}(t)$  is an output vector of the cantilever model.

$$\mathbf{A} = \begin{bmatrix} 0 & 1 & \dots & 0 & 0 \\ -\omega_1^2 & -\omega_1\gamma_1 & \dots & 0 & 0 \\ \vdots & \vdots & \ddots & \vdots & \vdots \\ 0 & 0 & 0 & 0 & 1 \\ 0 & 0 & 0 & -\omega_n^2 & -\omega_n\gamma_n \end{bmatrix}$$

$$\mathbf{B} = [0 \ \omega_1 \ \dots \ 0 \ \omega_n]$$

$$\mathbf{C} = [0 \ 1 \ \dots \ 0 \ 1]$$

$$\mathbf{D} = [0 \ 0 \ \dots \ 0 \ 0] \quad (7)$$

where the damping for all modes is  $\gamma_i = 1/Q$ . The quality factor  $Q$  of the cantilever in the air is usually between 10 and 500. Resonance frequency of each harmonic mode is  $\omega_i^2 = k/m_i^{eff}$ . Effective mass  $m_i^{eff}$  (Rast *et al.*, 2000) for harmonic mode is:

$$m_i^{eff} = \frac{3m}{\alpha_i^4} = \frac{3wtL\rho_0}{\alpha_i^4} \quad (8)$$

and for the stiffness of the cantilever stays:

$$k = \frac{Et^3w}{4L^3} \quad (9)$$

where  $w$  is width,  $t$  thickness,  $L$  length,  $E$  stiffness, and  $\rho_0$  is density of the cantilever.

### 3. THERMAL NOISE

In thermal equilibrium the thermal energy  $W$  given to the system depends only on the temperature of the system.

$$W = \frac{1}{2}k_B T \quad (10)$$

where  $k_B$  is Boltzmann constant and  $T$  is the system temperature. The calculation for multi mode model of the cantilever has been done by Hans-Jürgen Butt (Butt and Jäschke, 1995) and for each harmonic mode  $i$  has been calculated value of thermal noise displacement:

$$\hat{z}_i^2 = \frac{12k_B T}{k\alpha_i^4} \quad (11)$$

where  $k$  is the spring constant of the lever and  $\alpha_i$  is condition constant specifying each harmonic mode. Thermal energy is distributed to all harmonic modes and sum of the energy over all modes of the system has to be equal to total thermal energy of the system.

$$W = \sum_{i=1}^{\infty} W_i \quad (12)$$

where  $W_i$  is thermal energy for harmonic mode  $i$ . For each harmonic mode is the thermal energy:

$$W_i = \frac{6k_B T}{\alpha_i^4} \quad (13)$$

Simulated thermal noise is applied in form of displacement (force) onto the linear model of the cantilever as a white noise with normal distribution.

### 4. CANTILEVER IN INTERACTION WITH THE SURFACE

The cantilever is affected by many interacting forces while approaching and retracting from the surface of the sample (Gotsmann *et al.*, 1999). For weak forces measurements, the most important forces are van der Waals long distance attractive intermolecular force and short distance repulsive intermolecular forces. For our simulation we assume that the other forces (electrostatic, chemical) can be neglected by an appropriate design and construction of the AFM and they don't contribute in weak forces measurements. The model of the interaction forces is thus very simplified, but this minimized interaction is still very complex and many different behaviors of the lever can be observed. The field of attractive (negative) and repulsive (positive) forces  $F$  affecting the cantilever is shown in fig. 3.

For distances greater than interatomic spacing, the tip-surface separation distance  $z$  fulfil the condition  $z > a_0$ . The constant  $a_0$  is intermolecular distance and fully depends on material properties of the tip and the surface. For most of materials

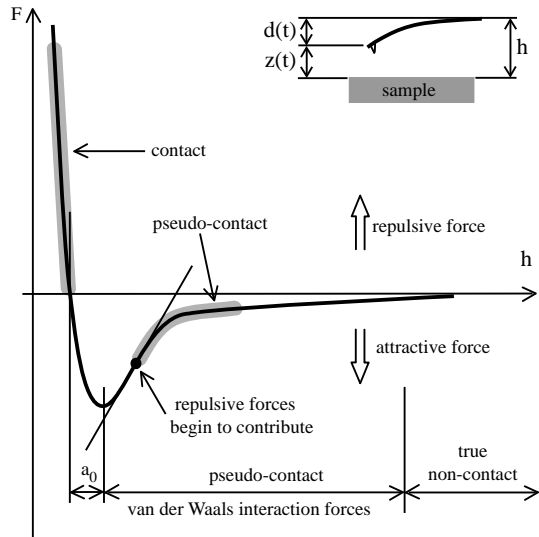


Fig. 3. Sketch of tip-sample interaction force

is  $a_0 \simeq 5\text{\AA}$ . Under this condition only attractive forces are present (there aren't any repulsive forces in the interaction). In most of the applications can be assumed, that the radius of the sample cylinder is significantly larger than the radius of the tip. The approximation of van der Waals interaction force can be simplified by Hamaker theory (Giessibl, 1997) and the expression of the attractive force between tip and surface is:

$$F_{vdW}(z) = -\frac{A_H R_s}{6z_0^2} \quad (14)$$

where  $R_s$  is tip radius and  $A_H$  is Hamaker constant. For distances in order of interatomic spacing, the tip-surface separation distance fulfil condition  $z \leq a_0$ . Direct overlap between electron wave functions (electron clouds) of the tip and the sample give important contribution and strong repulsive forces as a consequence of the Pauli principle are present. In the case of negligible energy dissipation in the tip-sample contact, a Derjaguin-Müller-Toporov (DMT) approximation can be used in the repulsive regime:

$$F_{DMT}(z) = -\frac{A_H R_s}{6a_0^2} + \frac{4}{3} E_{eff} \sqrt{R_s} (a_0 - z)^{3/2} \quad (15)$$

where  $E_{eff}$  is effective modulus of elasticity, see (Giessibl, 1997).

## 5. SIMULATION OF HIGHER HARMONIC MODES

The advantages of the multi mode model (7) are especially higher frequencies contribution in the cantilever movement. Computer simulation with the model excited only by thermal noise fig. 4 and comparison with the spectra measured on the real system fig. 5 with the same lever has been done.

Table 1 shows the properties which have been used for simulation and the information provided by manufacturer of the cantilever.

Table 1. Data-sheet properties of the contact silicon cantilever CSC12/50 (manufacturer UltraSharp) and table values for silicon material properties.

Description	Catalog			Used values
	min	typical	max	
Length, $L$ , [ $\mu\text{m}$ ]	-	350	-	350
Width, $w$ , [ $\mu\text{m}$ ]	-	35	-	35
Thickness, $t$ , [ $\mu\text{m}$ ]	0.7	1.0	1.3	1.1
Res. freq., $\omega$ , [kHz]	7.0	10	14	-
Spring con., $k$ , [N/m]	0.01	0.03	0.08	-
Density (Si), $\rho_0$ , [ $\text{kg}/\text{m}^{-3}$ ]	-	2330	-	2330
Stiffness (Si), $E$ , [GPa]	130	-	180	180

Computer simulations in Matlab/Simulink are very time consuming and because of this drawback the implemented model has only the first four modes. This simplification made the simulation and spectral analysis of the output signals reasonably fast. For the first four modes the resonance frequencies are shown in figure 4. The computed first resonance frequency is 11.8 kHz which fits into the limit values given by the data-sheet and the difference with its typical value is small. The detected resonance frequency of the real cantilever by microscope control system is 12.3 kHz. This difference could be caused by imperfect attachment of the chip with the cantilever to the bimorph driver of the AFM during the resonance frequency detection. Additionally the driving bimorph has its own resonant frequency. From measured frequency spectra figure 5 can be determined first resonant frequency at 9,68 kHz. The properties of the cantilever are slightly different to the values used in model and the cantilever has shape different from perfect rectangle. This is given by manufacturing the cantilever and its unperfect properties. Calculated spring constant  $k$  of the lever has a value 0.045N/m.

The contribution of high harmonic modes into the total displacement of the cantilever is displayed in figure 4. Dynamic system has been excited by thermal noise which is the natural noise that is present in all systems with nonzero temperature, commonly known as a Brownian motion of molecules of the system.

Table 2. Properties in simulation of the interaction between contact silicon cantilever CSC12/50 and silicon surface.

Description	Value
Hamaker constant (Si-Si), $A$ , [J]	$1.865 \cdot 10^{-19}$
Tip radius, $R$ , [nm]	10
Intermolecular Distance, $a_0$ , [nm]	0.38
Stiffness effective, $E_{eff}$ , [GPa]	10.2

The surface interaction model describing van der Waals attractive forces and repulsive forces, that

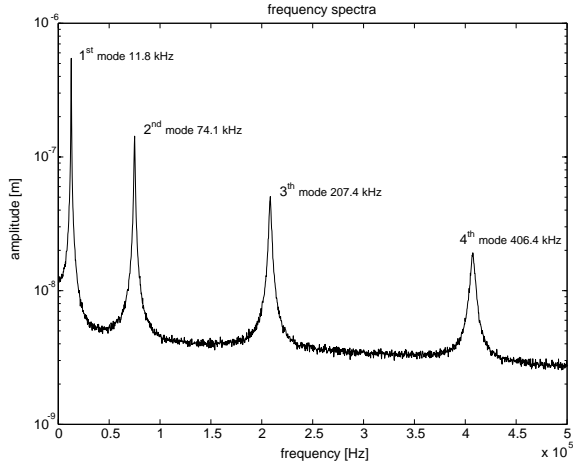


Fig. 4. Frequency spectra of the cantilever vibration excited by thermal noise, at the temperature  $T=295.15\text{K}$ .

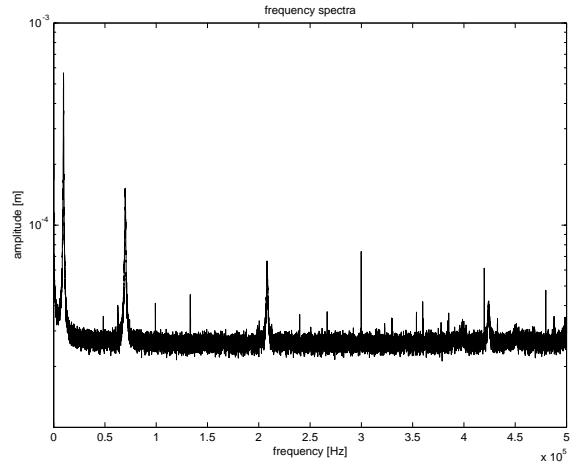


Fig. 5. Measured frequency spectra of the cantilever (CSC12/50 – manufacturer Ultra-Sharp) thermal vibrations with Digital Instruments AFM.

are between the tip and the surfaces, has been implemented into model of the cantilever which have been described above. Approximation of these interaction forces from equation 14 and 15 has been used. As a first step has been done amplitude calculation of interaction force as a function of separation distance, see figure 6. The simulation results and theoretical description given earlier are matching, see figure 3. The simulation has derivation discontinuity at the limit of intermolecular distance  $a_0$  due to separate models for attractive and repulsive force. This discontinuity doesn't cause any instabilities.

In second step has been simulated the approach to the surfaces with modelled cantilever and interaction forces. The approach curve is shown in figure 7. With decreasing separation distance between cantilever base and the surface  $h$  is increasing deflection of the lever  $d$ . At the distance  $h = 2.3\text{nm}$  the attractive van der Waals force is stronger then

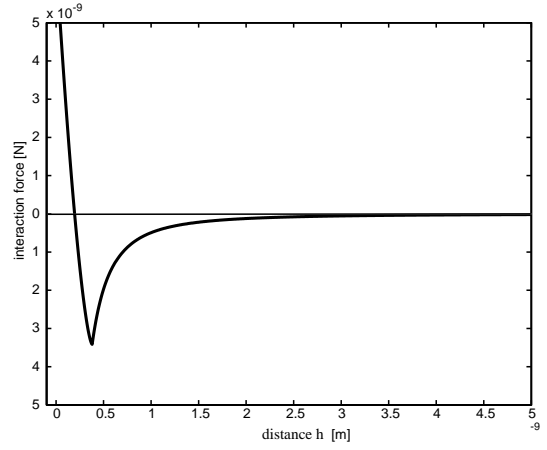


Fig. 6. Calculated intensity of interaction force between approaching object and surface.

the spring force of the cantilever and the lever "snaps" to the surface. When the tip approaches the surface closer, then intermolecular separation distance  $a_0$  repulsive forces begin to contribute and the cantilever settle at the intermolecular distance from surface. When the cantilever snaps to the surface all harmonic modes are excited due to very fast change in the cantilever position and speed. Transient vibration of the cantilever coupled to the surface are shown in figure 7.

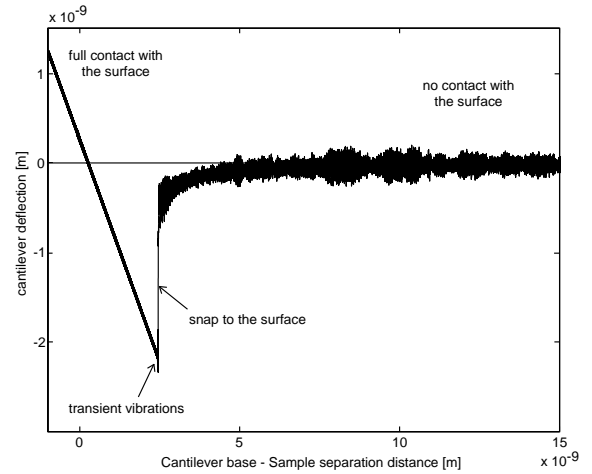


Fig. 7. Simulated approach curve of the cantilever to the surface. Thermal noise excitation is visible at the long separation distance.

## 6. CONCLUSION

The main aim, of this work was to develop multi mode cantilever model that is capable to describe the behavior of the real measuring system with good precision. Created model is taken into a consideration the influence of higher harmonics and their share on the total tip displacement of the cantilever. Simulated frequency spectra is fully fitting to theoretical expectation and has been

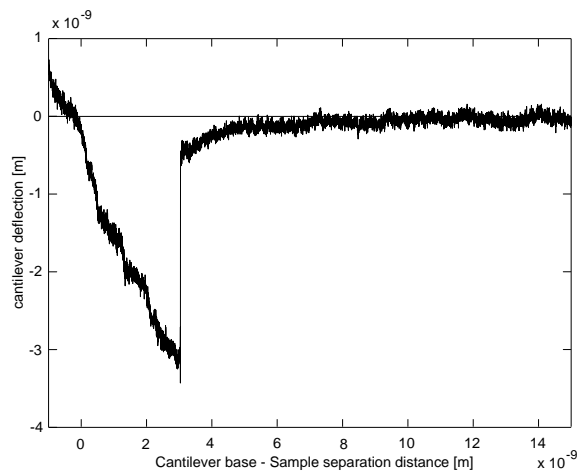


Fig. 8. Measured approach curve of the cantilever (CSC12/50 – manufacturer UltraSharp) to the surface with Digital Instruments AFM. Surface was silicon chip.

successfully confronted with measured data on the real system with a cantilever of same dimensions and properties. For a better understanding of the interaction and its impact on cantilever behavior a simple interaction model has been build using interaction forces approximations. Simulated approach curve has good match with measured approach curve on Digital Instrument atomic force microscope. The created model reach appropriate accuracy to be helpful tool for further design of control systems improving performance of the AFM.

#### REFERENCES

- Butt, Hans-Jürgen and Manfred Jaschke (1995). Calculation of thermal noise in atomic-force microscopy. *Nanotechnology* **6**, 1–7.
- Clough, Ray W. and Joseph Penzien (1993). *Dynamics of Structures*. McGraw-Hill, Inc.
- Giessibl, Franz J. (1997). Forces and frequency shifts in atomic-resolution dynamic-force microscopy. *Physical Review B* **56**(24), 16010–16015.
- Gotsmann, B., C. Seidel, B. Anczykowsky and H. Fuchs (1999). Conservative and dissipative tip-sample interaction forces probed with dynamic AFM. *Physical Review B* **60**(15), 11051–11061.
- M.Ashhab, M.V.Salapaka, M. Dahleh and I.Mezić (1999). Dynamical analysis and control of micro-cantilevers. *Automatica* **35**, 1663–1670.
- Rast, S., C. Wattering, U. Gysin and E. Meyer (2000). Dynamics of damped cantilevers. *Review of Scientific Instruments* **71**(7), 2772–2775.
- Stark, Robert W., Georg Schitter, Martin Stark, Reinhard Guckenberger and Andreas Stem-

mer (2004). State-space model of freely vibrating and surface-coupled cantilever dynamics in atomic force microscopy. *Physical Review B* **69**(8), 085412.